Electronic Structure of (n,0) Zigzag Carbon Nanotubes: Cluster and Crystal Approach

ARTICLE *in* THE JOURNAL OF PHYSICAL CHEMISTRY A · JANUARY 1998

Impact Factor: 2.69 · DOI: 10.1021/jp972300h

Electronic Structure of (*n*,0) Zigzag Carbon Nanotubes: Cluster and Crystal Approach

L. G. Bulusheva,*,† A. V. Okotrub,† D. A. Romanov,‡ and D. Tomanek§

Institute of Inorganic Chemistry SB RAS, Novosibirsk 630090, Russia, Institute of Semiconductor Physics SB RAS, Novosibirsk 630090, Russia, and Department of Physics and Astronomy, Michigan State University, East Lansing, Michigan 48824-1116

Received: July 15, 1997; In Final Form: November 12, 1997

We study the electronic structure of (*n*,0) zigzag carbon nanotubes by means of two complementary numerical methods. Using the semiempirical PM3 method, we carry out quantum-chemical calculations for tube fragments of different symmetry and size, which represent these tubes. Using the tight-binding method, we proceed in parallel to determine the band structure of these tubes. The effect of cluster size on the structure of frontier orbitals and on the cluster stability is investigated for the (6,0) tube. We show that the highest occupied molecular orbitals (HOMOs) and the lowest unoccupied molecular orbitals (LUMOs) of the (*n*,0) tube fragments are localized on the edge atoms. The comparison between the band structure of the (6,0) tube and the molecular orbitals of the (6,0) tube fragment with 13 carbon hexagons along the tube axis indicates that the spatial structure of the HOMO′s and the LUMO′s directly corresponds to that of the Bloch wave functions of occupied and unoccupied π bands near the Fermi level.

Introduction

The discovery of fullerenes has stimulated the investigations of various cage forms of carbon. Perhaps most prominent are carbon nanotubes, single-wall and multiwall structures 1000−10000 Å long and 10−100 Å wide. Multiwall nanotubes are found in the negative electrode deposit formed in the process of arc evaporation of graphite.[1−3] Both multiwall and single-wall carbon nanotubes are also synthesized in catalytic reactions.[4−6] From the microscopic viewpoint, such systems are constructed from rolled sheets of connected carbon hexagons. The orientation of the hexagons with respect to the tube axis determines the type of the nanotube, specified by the diameter, the chirality, and the handedness. Compared to graphite, carbon hexagons in nanotubes are distorted owing to the small diameter and chiral structure of the tube.

Since the first moment when carbon nanotubes were discovered, their atomic and electronic structures have been intensively explored.[7,8] Particularly, some interesting rules have been found, which correlate the atomic structure with the electronic structure of the nanotubes and their electrophysical properties.[9−11] Quasi-one-dimensional and chiral character of the electron states in nanotubes affect substantially most of their electrophysical properties (such as conductivity, galvanomagnetic and photoelectric characteristics, the static and high-frequency polarizability, etc.). These, in turn, determine the prospect for their use in various areas of nanoelectronics.

The reactivity of these carbon compounds is also determined by their unique spatial structure. In this connection, the local structural factors seem to be most important for effects such as the difference of chemical interactions with the outer and inner surfaces of the nanotubes, or the distortion of carbon hexagons. Controllable use of these chemical properties for the modification of the atomic and electronic structure of nanotubes by means of intercalation and/or chemisorption would allow us to effectively modulate the mentioned electrophysical effects.

The electronic characteristics of the nanotubes have been investigated theoretically mostly by means of numerical band-structure calculations.[12−14] Such results yield dispersion relations for the individual electronic bands, i.e., the dependency of the electron energy in a particular subband on the wave vector in the one-dimensional Brillouin zone. More recent variants of the band-structure calculations can also yield the interband matrix elements of the velocity operator and hence determine the kinetic behavior of the one-dimensional electrons.

However, no less interesting is another aspect of the nanotube electronic structure, namely, the structure of the chemical bonds. This is given by the local spatial structure of the orbitals. To describe the state of individual atoms and to get chemically significant information, it seems more natural (and more correct) to use quantum-chemical methods, which are particularly suited for determining the local properties of an investigated system. These methods were originally designed to describe finite systems. So any extension of the obtained results to the case of infinite system faces certain difficulties and must be performed with care. In particular, one has to properly choose the representative cluster and to separate bulk from surface effects in the results. Cluster methods allow us to study the electronic structure of real physical objects, in particular, to estimate how the surface of a cluster affects its reactivity and electrophysical properties.

In this paper we present results of quantum-chemical calculations for fragments of (*n*,0) nanotubes. Our goals are to determine the effects of the frontier electron states, i.e., the HOMO and the LUMO, on the growth, destruction, and the reactivity of the nanotubes and to find the correlation between the results of the cluster approach and the band approaches to calculating the electronic structure of nanotubes.

(*n*,0) Nanotubes

From the theoretical viewpoint, the simplest nanotubes have a single wall. There are two types of achiral single-wall nanotubes. In the (*n*,*n*) "armchair" nanotubes,[15] two sides of each hexagon are perpendicular to the tube axis. In the (*n*,0)

† Institute of Inorganic Chemistry.
‡ Institute of Semiconductor Physics.
§ Michigan State University.

S1089-5639(97)02300-1 CCC: $15.00
Published on Web 01/22/1998

"zigzag" nanotubes, two sides of each hexagon are parallel to the tube axis. In the pioneering theoretical treatments of these systems[16,17] the electronic structure of both types was analyzed using the so-called "folded zone" model framework. This model suggests a simple recipe to obtain the basic features of the tube band structure by cyclic quantization of the graphene sheet quasi-momentum component corresponding to the electron motion along the tube circumference. The quantization condition defines an array of equidistant lines in the hexagonal Brillouin zone of the graphene sheet. These lines are parallel to the tube axis, and each of them corresponds to a one-dimensional subband. The valence and conduction bands of the graphene sheet are known to "touch" at the corners of the hexagonal Brillouin zone, often labeled as the K point. The gap between the valence and the conduction band is proportional to the distance from the K point in its vicinity. In particular, (n,n) and (3n,0) tubes have a zero-width gap, i.e., are metals. These theoretical results for (n,n) tubes have been later confirmed by direct energy band calculations for thin nanotubes[18] and appear to agree with the experimental data for the (10,10) tube.[19] On the other hand, (n,0) tubes have not been observed as often as (n,n) tubes. Since total energy calculations do not indicate the (n,0) tubes to be unstable, these tubes are naturally the first candidate for a complementary quantum-chemical cluster analysis.

The electronic structure of the carbon nanotube fragment and, hence, the physical and chemical properties of the cluster depend strongly on the cluster size and point-group symmetry. The symmetry properties of a given nanotube fragment are determined by the number of hexagons along the tube axis, N, being even or odd and the number of hexagons along the tube circumference, n, being even or odd. The four possible combinations of these numbers give two different kinds of point groups (D_{nh} and D_{nd}), which, in turn, determine the differences in the structure of molecular orbitals, obtained from quantum-chemical calculations.

Calculations

For numerical calculation of the electronic structure of the nanotube fragments we have used the MNDO semiempirical method,[20] which belongs to the group of SCF-MO-LCAO methods. In this method, only valence electrons are taken into account, and the three- and four-center integrals are omitted. By use of the spatial anisotropy of p orbitals in two-electron integrals calculations, this method allows us to describe correctly the repulsion of lone electron pairs. The choice of the phenomenological parameters on the basis of experimental data helps us to automatically include correlation effects. Calculations were carried out using the PM3 parametrization[21] and the GAMESS package.[22] The SCF convergence criterion was 10^{-8} for total-energy changes and 10^{-5} for charge-density changes between two subsequent cycles.

Band structure calculations of (n,0) tubes were performed using the tight-binding Hamiltonian, with a universal set of first and second nearest-neighbor hopping integrals that reproduce various carbon structures, including graphite.[23,24]

Structure of (6,0) Carbon Nanotubes

To study the dependency of the electronic structure of (n,0) nanotube fragments on their size, we have considered fragments of the (6,0) tube. The (6,0) carbon tube seems to have the lowest experimentally realizable diameter. As shown previously,[25,26] tubes with a smaller diameter are thermodynamically unstable. We considered (6,0) tube fragments of different length. The dangling bonds at the ends of the nanotube fragments were saturated by hydrogen atoms. The structural unit of the tube is the distorted carbon hexagon. In the calculation, all carbon−carbon bonds were assumed to be of the same length: 1.4 Å. The distance between third-neighbor carbon atoms along the tube circumference is 2.39 Å. This structure has been previously obtained from geometry optimizations, based on molecular mechanics modeling using the MM+ force field, of a nanotube fragment with 13 hexagons along the tube axis.[27] The point-group symmetry of the (6,0) nanotube fragment is determined by the number N of carbon hexagons along the tube axis. Nanotube fragments with odd N belong to the group D_{nh}, whereas nanotube fragments with even N belong to the group D_{nd} (see Figure 1).

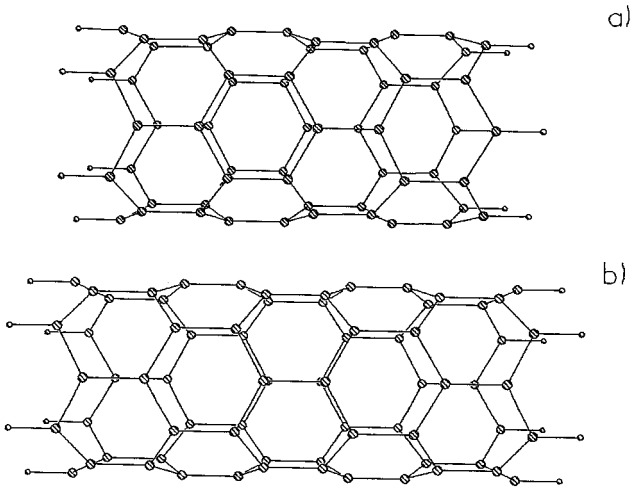

Figure 1. (6,0) nanotube fragments of D_{6d} (a) and D_{6h} (b) symmetries.

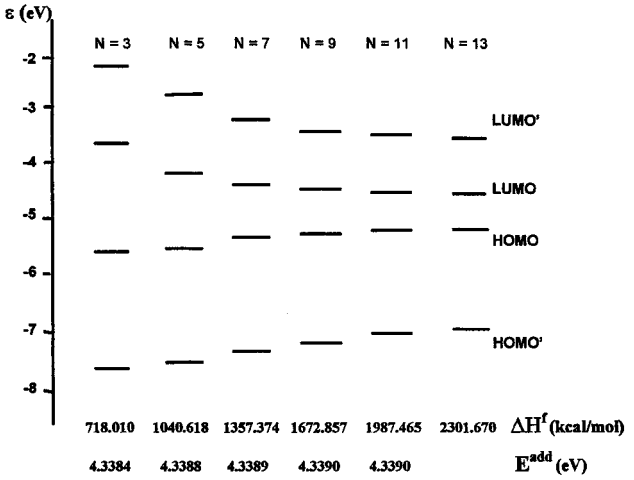

Figure 2. Calculated energy of frontier orbitals, the heat of formation (ΔH^f), and the energy required to join an additional carbon atom (E^{add}) to fragments of the (6,0) tube with N hexagons in axial direction.

Nanotube Fragments of D_{6h} Symmetry

We have considered nanotube fragments with $N = 3$, 5, 7, 9, 11, and 13. Our results for the heat of formation of the nanotube fragments, the energy required to adsorb an additional carbon atom at the edge, and the energies of the frontier orbitals are presented in Figure 2. The considerable energy difference between the nanotube fragments with $N = 3$ and $N = 5$ is caused by the fact that in the former case the boundary atoms affect strongly the central part of the nanotube fragment. The energy required to incorporate an additional atom remains practically

constant between $N = 9$ and $N = 13$. The obtained numerical results allow us to figure out the screening length of the tube-end defects that affect the local electronic structure inside the tube. This length corresponds to four hexagons. Therefore, the nanotube fragment with $N = 9$ is quite sufficient for modeling the energy characteristics of an infinite tube.

The nanotube fragments with $N = 3$, 7, and 11 have their HOMOs of b_{1g} symmetry and LUMOs of b_{2u} symmetry. The HOMOs and LUMOs in nanotube fragments with $N = 5$, 9, and 13 are of b_{1u} and b_{2g} symmetries, respectively. The spatial structure of these molecular orbitals consists mainly of the orbitals of carbon atoms belonging to the ends of the tube that are saturated by auxiliary hydrogen atoms. These atomic orbitals are radially directed (π-like orbitals). Such HOMO and LUMO orbitals are expected in finite clusters but have little to do with the electronic properties of infinite tubes. On the other hand, these orbitals are supposed to play a crucial role in processes taking place at the ends of real nanotubes, such as tube growth or oxidation. The physical and chemical properties of infinitely long tubes (i.e., conductivity, reactivity, etc.) will be determined by the top of the valence and the bottom of the conduction bands (corresponding to HOMO and LUMO orbitals for an infinitely long tube). We expect the HOMO−LUMO gap to decrease with increasing tube-fragment size. In the following, we denote these HOMO and LUMO orbitals for an infinitely long tube by HOMO′ and LUMO′. These orbitals for the infinite (6,0) tube are of e-type and correspond to occupied and unoccupied π bands near the Fermi level. From the point of view of band-structure calculations, the conduction properties of nanotubes are determined by the fundamental energy gap.[12,28] Our cluster calculations cannot describe solid-state properties such as transport. Moreover, cluster calculations overestimate the fundamental gap. The dependency of this energy gap on the length of the nanotube fragments under consideration is shown in Figure 2. Increasing the fragment size reduces the gap. However, changes in the HOMO−LUMO gap diminish quickly with increasing fragment size and become negligibly small when comparing this quantity in $N = 11$ and $N = 13$ tube fragments. We expect a gap exceeding ~1−3 eV in very large tube fragments, which (with the exception of the impurity states inside the gap, introduced by the finite size) should be compared to the width of the fundamental gap obtained from band-structure calculations.

The tight-binding result for (6,0) tube and the result of PM3 calculation of the (6,0) nanotube fragment with $N = 13$ are compared in Figure 3. The molecular levels of the nanotube fragment, formed from 2p atomic orbitals (AOs) of carbon atoms, are presented on the left-hand side. These molecular orbitals can be separated into two basic blocks. The block consisting of r orbitals (which provide π interactions between carbon atoms) lies at higher energy. The other block, consisting of τ orbitals (which provide the σ interactions between carbon atoms), lies at lower energy. The dispersion curves $E(k)$ for occupied energy bands, formed from 2p AOs of carbon atoms, are drawn in the right part of Figure 3. The bands are also clearly divided into two blocks, the block of π bands and the block of σ bands. The corresponding bandwidths are well-correlated with the widths of the r- and τ-orbital energy blocks shown on the left. Figure 3 shows also that the energy levels corresponding to the HOMO of the nanotube fragment have no counterpart in the infinite (6,0) tube. We must exclude this level from our discussion when comparing results of cluster and band-structure calculations. In particular, we find that the spatial structure of the LUMO′ (e_{2g}) and HOMO′ (e_{2u}) orbitals

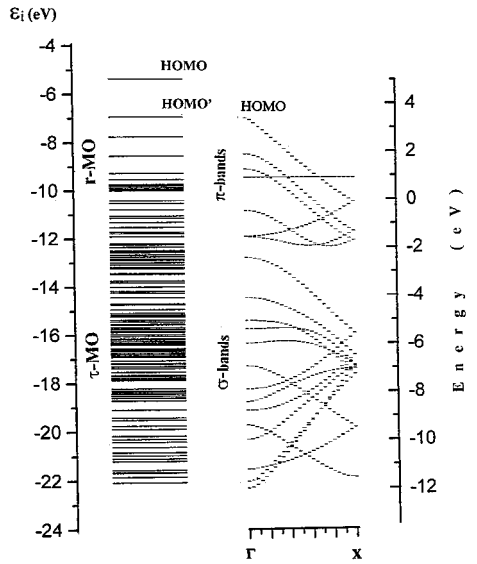

Figure 3. Comparison between the molecular levels of (6,0) tube fragments with $N = 13$ hexagons in axial direction (left) and band structure of the (6,0) tube (right).

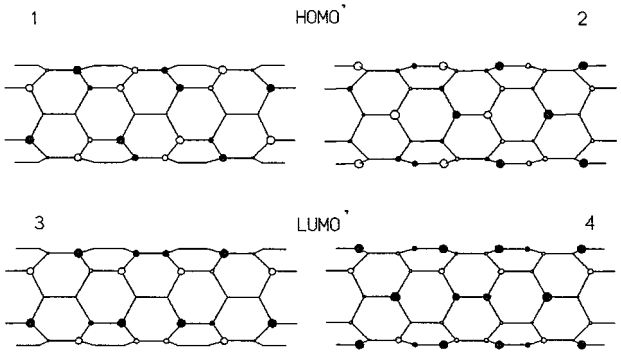

Figure 4. Electronic states at the top of the valence band (HOMO′) and bottom of the conduction band (LUMO′) of the (6,0) tube.

corresponds to that of Bloch wave functions of the occupied and unoccupied π bands near the Fermi level.

We show the structure of these r orbitals for carbon atoms at the fragment surface in Figure 4. White circles denote AOs directed toward the tube axis, black circles AOs directed outward. The HOMO′ and the LUMO′ contain one orbital with clearly visible stripe character. We find four stripes containing carbon atoms that have zero contribution to their charge density from these orbitals. The chains of carbon atoms between these stripes contain atoms, on which these states are predominantly localized. This analysis of the electronic structure of the (6,0) nanotube fragments demonstrates that fragments with $N = 5$ already show the stripe structure in their molecular orbitals. Consequently, this cluster size is sufficient for a quantitative discussion of the character of electron wave functions in an infinite tube. Previously, we had also found the stripe structure in the HOMOs and LUMOs of (n,n) tubes, in which case the stripes were of perimetric belt type.[27]

Nanotube Fragments of D_{6d} Symmetry

It is usual in self-consistent calculations to estimate the accuracy of the wave functions and corresponding energies. The solution of the Hartree−Fock equation is regarded as self-consistent if for two consequent iterations the variation of the total energy of the system is less than a given (small) quantity δ, whereas the variation of the charge density is less than another

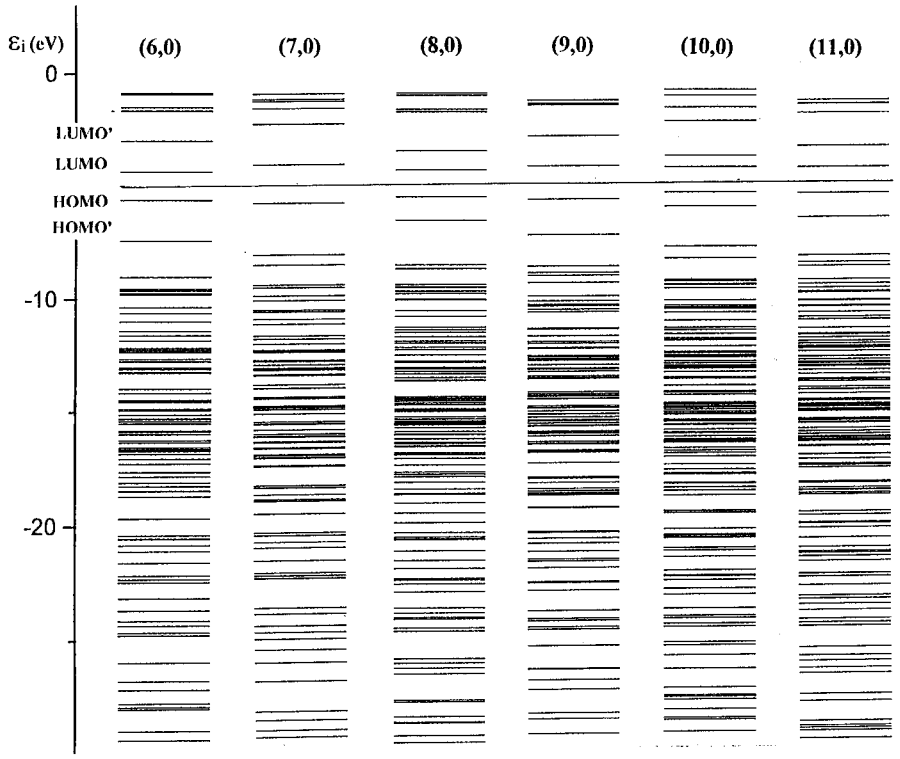

Figure 5. Electronic eigenvalues of calculated fragments of (*n*,0) tubes, with $n = 6, ..., 11$.

quantity δ'. In calculations of (6,0) tubes with even-numbered N (i.e., for tube fragments of D_{6d} symmetry) we could not achieve charge-density convergence for $\delta' < 10^{-2}$. Consequently, the quality of our wave functions is not sufficient for quantitative discussions.

A more detailed examination shows that the LUMO and HOMO of these nanotube fragments are energetically degenerate and belong to the irreducible representation e_3. In other words, the HOMO of these nanotube fragments is half-occupied. The mentioned LUMO and HOMO, as well as these orbitals in D_{6h} nanotube fragments, consist mainly of 2p AOs of the edge atoms. By virtue of the symmetry operations of the point group D_{6d}, such orbitals have to be doubly degenerate. The total number of electrons in the system is not sufficient to fill this orbital completely. The unpaired spins result in a net dipole moment and prevent the self-consistent calculation from converging. However, adding two extra electrons to the system (e.g., by intercalation) results in zero net dipole moment for the completely filled HOMO, and the self- consistent computation converges. From this consideration we can conclude that the charge-neutral nanotube fragments of D_{6d} symmetry are unstable. We would, however, expect a stabilization of this system by a symmetry-lowering Jahn−Teller distortion. The structures of the HOMO and LUMO orbitals in nanotube fragments of D_{6d} symmetry appear to be similar to those of D_{6h} nanotube fragments.

Electronic Structure of (*n*,0) Tubes

To study the dependency of the electronic structure of (*n*,0) tubes on the number of hexagons *n* along their perimeter, we considered nanotube fragments with the same number of hexagons in the axial direction. For the latter quantity we used $N = 5$, i.e., we considered nanotube fragments of D_{nh} symmetry. We performed quantum-mechanical calculations for (*n*,0) nanotube fragments with $n = 6, ..., 11$. Electron level diagrams for these nanotube fragments are presented in Figure 5. For all the considered (*n*,0) nanotube fragments the electron density of the HOMO and LUMO is localized on those carbon atoms at the edge that are connected to hydrogen atoms. In fragments of (6,0), (8,0), and (10,0) nanotubes, the LUMO and HOMO are nondegenerate. In fragments of (7,0), (9,0), and (11,0) nanotubes, these orbitals are doubly degenerate. The latter fact seems to be caused by the number of hexagons along the tube perimeter being odd. The HOMO′ and LUMO′ states in nanotube fragments of (6,0)−(11,0) tubes have doubly degenerate orbitals of r type. The (*n*,0) tubes we considered split naturally into two groups, namely, tubes with an even number of hexagons along the tube perimeter (even *n*) and tubes with an odd value of *n*. In tubes with both an even-valued and odd-valued *n* (Figure 5), the energy gap between the HOMO′ and the LUMO′ decreases with increasing tube diameter, though the gap is larger in tubes with an odd-valued *n*. As we know from cluster calculations, the HOMO−LUMO gap correlates with the stability of the nanotube fragment. We conclude that tubes with an odd-valued *n* should be synthesized in larger abundance under thermodynamically controllable conditions.

The HOMO′ structures for the (7,0)−(11,0) tubes are shown in Figure 6. The character of the interaction between carbon atoms in the HOMO′ of these tubes is similar to that of (6,0) tube. As in the latter case, we observe bonding character in pairs of atoms bonded along the tube perimeter, and antibonding character in bonds along the tube axis. Stripes of carbon sites, which have zero contribution to their charge density from this MO, can be seen in each of the component orbitals of the HOMO′ set for the (7,0), (8,0), (10,0), and (11,0) tubes. For the (6,0) and (9,0) tubes, on the other hand, only one component of the HOMO′ orbital set shows an obvious stripe character. The stripes in these tubes are distributed symmetrically, and all of them are half a hexagon wide. In (9,0) nanotube fragments, we observe six stripes of carbon atoms with zero electron density that connect to chains, similar to the results discussed for the (6,0) tube.

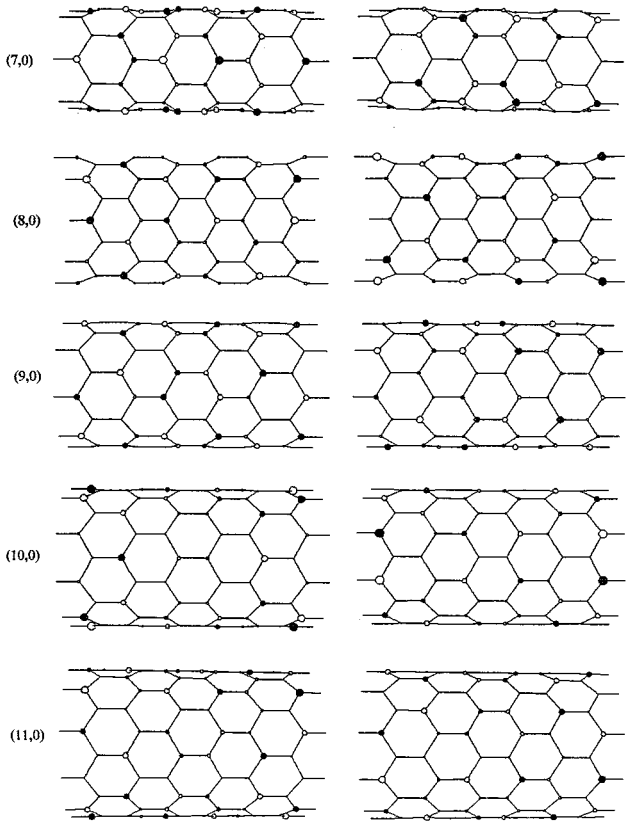

Figure 6. Structure of the electronic states at the top of the valence band (HOMO′) in fragments of (*n*,0) tubes, with $n = 7, ..., 11$.

Discussion

Carbon nanotubes are commonly treated as rolled graphene sheets. For tubes of large diameter (exceeding 10 Å), distortions of the constituting hexagons can be regarded as negligible. This is why the tube band structures seem to be closely related to that of graphite.[29] As for the quantum-chemical cluster calculations, the representative nanotube fragment of the graphene sheet has to have D_{6h} symmetry. On the other hand, an unfolded tube is a sheet of D_{2h} symmetry, the electronic structure of which should be different from a finite graphite flake of D_{6h} symmetry, at least for symmetry reasons. This naturally motivated us to investigate the evolution of the HOMO and LUMO structures, since with increasing length the unfolded nanotube fragment changes its point-group symmetry from D_{6h} to D_{2h} to, finally, to D_{nh}.

For this purpose we considered first the $C_{96}H_{24}$ flake of D_{6h} symmetry. The HOMO and LUMO in this nanotube fragment are e-type; their structures are shown in Figure 7. One of these orbitals shows obvious stripes. We have then considered the $C_{78}H_{22}$ flake of D_{2h} symmetry. The symmetry reduction splits energetically the HOMO. The structure of this MO corresponds to one of the orbital components of the $C_{96}H_{24}$ HOMO set, shown in Figure 7.1, and consists of carbon-atom chains establishing stripes of alternating zero and nonzero charge density according to the contribution of a particular orbital to a given site. Once the sheet is rolled to form an (*n*,0) tube so that two sides of each carbon hexagon are oriented axially, then the mentioned stripes will also align axially. On the other hand, if the sheet is rolled to form an (*n*,*n*) tube, where two sides of each carbon hexagon are oriented normal to the tube axis, then the stripes run along the perimeter. This strictly corresponds to the electronic structure calculations of (*n*,0) tubes discussed above and to calculations of (*n*,*n*) tubes in ref 27. The HOMO

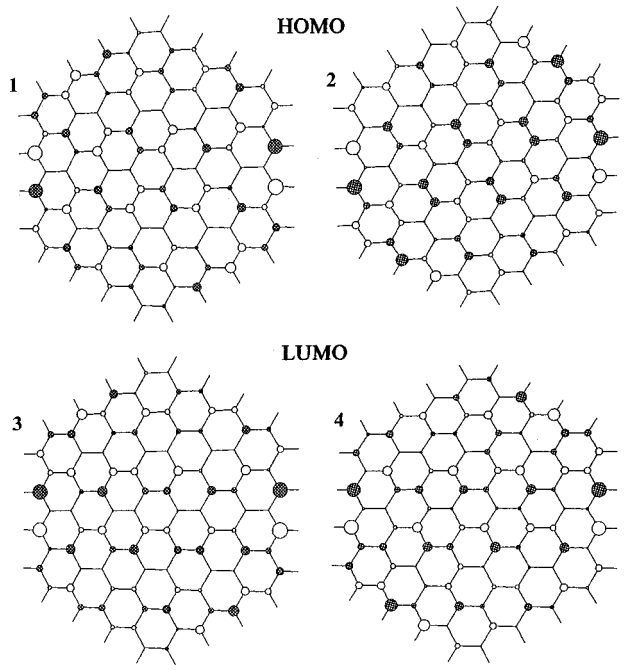

Figure 7. Structure of the HOMO and LUMO states in a graphite flake of D_{6h} symmetry, a fragment of an infinite-diameter tube.

of (*n*,*n*) tubes is singly degenerate, in agreement with results of band-structure calculations.[18] The HOMO of (*n*,0) tubes, owing to symmetry reasons, only shows the stripe character if it is doubly degenerate. The results of our band calculations also show the highest occupied band of (*n*,0) tubes to be of e symmetry.

The dispersion curves of the (*n*,0) tubes with $n = 6, ..., 11$ are shown in Figure 8. This tube family splits into three groups. The (3*n*,0) tubes have vanishing energy gaps. The gap increases in $(3n + 1, 0)$ and in $(3n + 2, 0)$ tubes. Consequently, (6,0) and (9,0) tubes will likely show metallic conductivity, similar to graphite. Comparing the HOMO structure of graphite flakes, on the basis of our calculations for flat nanotube fragments, with the HOMO′ structure of (*n*,0) tube fragments with $n = 6, ..., 11$, we see a similarity between the graphite flakes and only the (6,0) and (9,0) tubes. One of the degenerate HOMO′ orbitals in these tubes shows a regular stripe pattern due to chains of carbon atoms, the AOs of which have zero character in the HOMO′, and chains of atoms that do contribute to the HOMO′ wave function. Band-folding arguments mentioned above, supported by the HOMO electronic structure of graphite flakes shown in Figure 7.1, suggest that such a regular stripe structure of the HOMO is possible only in (3*n*,0) tubes.

Rolling of a graphene sheet into a cylinder changes the hybridization of the carbon atoms. In graphite, π orbitals are represented by the lone 2p(C) AOs normal to the graphene plane, and σ orbitals are linear combinations of in-plane 2s(C)- and 2p(C) AOs. In carbon nanotubes, the radial orbitals, with a radial node in the cylinder, are analogous to the lone π orbitals of graphite yet contain an admixture of 2s(C) AOs. This changes the character of the frontier orbitals of carbon nanotubes in comparison with those of graphite, in particular for nanotubes with a small radius. Our calculations of (6,0) tube fragments show that 2s(C) AOs contribution in the HOMO′ (LUMO′) of these systems is roughly 1%. Owing to the changed s−p hybridization, the radial states have a different weight inside and outside the tube. Hence, the reactivity of inner and outer surfaces of single tubes will be different. The charge-density distribution of frontier orbitals in (*n*,0) nanotube fragments is

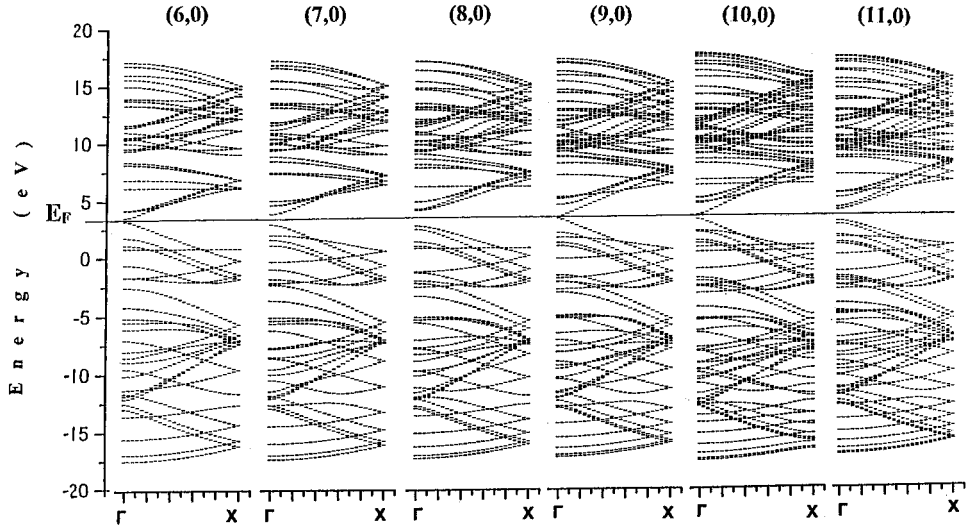

Figure 8. Band structure of (n,0) tubes, with $n = 6, ..., 11$.

shifted from the inside to the outside of the tube. As a result, tube surfaces are polarized in the radial direction, resulting in a nonzero electric field in the radial direction. We expect the inner surface to behave like an acceptor and to preferentially bind donor elements, such as metals. The outer surface should have donor properties and be more reactive with halogens.

Tubule Growth

Presently available data suggest that (n,0) nanotubes are far less abundant than the (n,n) nanotubes that are routinely synthesized catalytically by laser vaporization of graphite or by decomposition of hydrocarbons. Tubes observed in the carbon deposit of arc-discharge reactors are often chiral. Since the chiral angle in these latter tubules is 3−12°,[8] their atomic structures are rather similar to those of (n,0) tubules. The question of interest is whether this chirality occurs because of some thermodynamic reason or whether it is determined by particular growth kinetics. Then, whatever the origin of the chirality is, it would be interesting to intentionally vary the chiral angle and, particularly, to produce achiral (n,0) tubes by changing the synthesis conditions such as electric and/or magnetic fields in the reactor, adding/modifying the catalyst, etc. From this viewpoint, our results for the frontier orbitals are most important. The frontier nature of these orbitals is twofold. Spatially, they are localized at the tube ends. In the energy scale, they occur inside the fundamental gap of the infinite tube. As discussed above, these orbitals are essentially different in the cases of tubes with an even and with an odd number of hexagons along the tube axis N.

In tubes with odd-valued N, the frontier orbitals correspond to the HOMO and LUMO of infinite tubes. Consequently, the adsorption of carbon atoms (or atoms of other elements) takes place at the ends of the tube and results in net growth of the tube. However, as soon as one more layer (or ring) is completed at the tube end, N increases by 1 and becomes even. As discussed above, such tubes with an even-valued N are unstable when charge-neutral but become stable when carrying an excess charge of $-2e$. In the case of electron deficiency (the net electric charge being $+2e$), the boundary states are absent, and the tubule reactivity decreases. We conclude that continuing growth of (n,0) nanotubes requires a net excess charge, which could be provided from the cathode of the carbon-arc apparatus or by using alkali or alkali-earth metals as catalysts.

Since carbon tubes are known to grow on the cathode during the carbon-arc discharge process, the reasoning presented above should suggest the formation of (n,0) nanotubes under these conditions. Indeed, the (n,m) tubes generated in this way are characterized by m typically much smaller than n, corresponding to a small chiral angle. The nonzero value of the chiral angle is linked to growth kinetics, since the fastest growth is expected near the "step" at the growing edge. From the chemical viewpoint, the most interesting feature of the frontier orbitals is that they are of r type. This means that these orbitals do not take part in the radical chemisorption reaction. Their role is nevertheless crucial, since they are associated with all the carbon atoms that adsorb at the entire surface of the tubule and then diffuse to either end. Thus, the very existence of the frontier orbitals makes the oxidation and chemical destruction processes take place at the tube ends.[30,31]

Conclusions

We used side-by-side a band-structure and a quantum-chemical approach to calculate the dependency of the electronic structure of (n,0) nanotubes, in particular the structure of the frontier MOs, on n. The electronic structure of nanotube fragments is shown to depend sensitively on the number of hexagons in the axial direction N and along the perimeter n being even- or odd-valued. Nanotube fragments of D_{nd} symmetry (with an even number of hexagons in the axial direction) are thermodynamically unstable when the charge is neutral. We believe that the presence of carbon nanotubes with a structure close to that of (n,0) tubes results from a net negative charge provided by the cathode in the carbon arc. The HOMO structure of (n,0) nanotube fragments depends on the symmetry of the fragment but is localized on the edge atoms. This reactive frontier orbital is responsible for the tube growth, resulting from carbon adsorbed on the walls diffusing to and adsorbing on the exposed edge.

A comparison between results of band structure and cluster techniques shows that the occupied and unoccupied Bloch states of π character, found near the Fermi level of (n,0) tubes, correspond to the HOMO′s and LUMO′s of carbon nanotube fragments. The HOMO′ and LUMO′ of (3n,0) tube fragments correspond to the HOMO and LUMO of flat graphite flakes of D_{6h} symmetry, which is the reason for the metallic character of these tubes.

Acknowledgment. The work has been financially supported by the program "Actual directions in physics of condensed

states", specifically, "Fullerenes and atomic clusters", No. 94055 and "Surface atomic structures", No. 95-2.11.

References and Notes

(1) Iijima, S. *Nature* **1991**, *354*, 56.
(2) Ebbesen, T. W.; Ajayan, P. M. *Nature* **1992**, *358*, 220.
(3) Ando, Y.; Iijima, S. *Jpn. J. Appl. Phys.* **1993**, *32*, L107.
(4) Ge, M.; Sattler, K. *J. Phys. Chem. Solids* **1993**, *54*, 1871.
(5) Ge, M.; Sattler, K. *Mater. Res. Soc. Symp. Proc.* **1994**, *349*, 313.
(6) Endo, M.; Takeuchi, K.; Igarashi, S.; Kobory, K.; Shiraishi, M.; Kroto, H. W. *J. Phys. Chem. Solids* **1993**, *54*, 1841.
(7) Tsang, S. C.; de Oliveira, P.; Davis, J. J.; Green, M. L. H.; Hill, H. A. O. *Chem. Phys. Lett.* **1996**, *249*, 413.
(8) Okotrub, A. V.; Romanov, D. A.; Chuvilin, A. L.; Shevtsov, Yu. V.; Gutakovskii, A. K.; Bulusheva, L. G.; Mazalov, L. N. *Phys. Low-Dimens. Struct.* **1995**, *8/9*, 139.
(9) Romanov, D. A.; Kibis, O. V. *Phys. Lett. A* **1993**, *178*, 335.
(10) Mintmire, J. W.; Robertson, D. H.; White, C. T. *J. Phys. Solids* **1993**, *54*, 1835.
(11) Hiura, H.; Ebbesen, T. W.; Tanigaki, K.; Takahashi, H. *Chem. Phys. Lett.* **1993**, *202*, 509.
(12) Hamada, N.; Sawada, S.; Oshiyama, A. *Phys. Rev. Lett.* **1992**, *68*, 1579.
(13) Akagi, K.; Tamura, R.; Tsukada, M. *Phys. Rev.* **1996**, *B53*, 2114.
(14) Chico, L.; Crespi, V. H.; Benedict, L. X.; Louie, S. G.; Cohen, M. L. *Phys. Rev. Lett.* **1996**, *76*, 971.
(15) Dresselhaus, M. S.; Dresselhaus, G.; Saito, R. *Phys. Rev.* **1992**, *B45*, 6234.
(16) Jishi, R. A.; Venkataraman, L.; Dresselhaus, M. S.; Dresselhaus, G. *Chem. Phys. Lett.* **1993**, *209*, 77.
(17) Lin-Chung, P. J.; Rajagopal, A. K. *J. Phys.: Condens. Matter* **1994**, *6*, 3697.
(18) Mintmire, J. W.; Dunlap, B. I.; White, C. T. *Phys. Rev. Lett.* **1992**, *68*, 631.
(19) Thess, A.; Lee, R.; Nikolaev, P.; Dai, H.; Petit, P.; Robert, V.; Xu, C.; Lee, Y. H.; Kim, S. G.; Rinzler, A. G.; Colbert, D. T.; Scuseria, G. E.; Tomanek, D.; Fischer, J. E.; Smalley, R. E. *Science* **1996**, *273*, 483.
(20) Dewar, M. J. S.; Thiel, W. *J. Am. Chem. Soc.* **1977**, *99*, 4899.
(21) Steward, J. J. P. *J. Comput. Chem.* **1989**, *10*, 209.
(22) Schmidt, M. W.; Baldridge, K. K.; Boatz, J. A.; Elbert, S. T.; Gordon, M. S.; Jensen, J. H.; Kosoki, S.; Matsunaga, N.; Nguyen, K. A.; Su, S. J.; Windus, T. L.; Dupluis, M.; Montgomery, J. A. *J. Comput. Chem.* **1993**, *14*, 1347.
(23) Tomanek, D.; Schluter, M. A. *Phys. Rev. Lett.* **1991**, *67*, 2331.
(24) Tomanek, D.; Louie, S. G. *Phys. Rev.* **1988**, *B37*, 8327.
(25) Lucas, A. A.; Lambin, P. H.; Smalley, R. E. *J. Phys. Chem. Solids* **1993**, *54*, 586.
(26) Sawada, S.; Hamada, N. *Solid State Commun.* **1992**, *83*, 917.
(27) Okotrub, A. V.; Romanov, D. A.; Bulusheva, L. G. *Recent Adv. Chem. Phys. Fullerenes Relat. Mater.* **1996**, *3*, 959.
(28) Dresselhaus, M. S.; Dresselhaus, G.; Saito, R. *Solid State Commun.* **1992**, *84*, 201.
(29) Blase, X.; Benedict, L. X.; Sherley, E. L.; Louie, S. G. *Phys. Rev. Lett.* **1994**, *72*, 1878.
(30) Tsang, S. C.; Harris, P. J. F.; Green, M. L. H. *Nature* **1993**, *362*, 520.
(31) Ajayan, P. M.; Ebbesen, T. W.; Ichihashi, T.; Iijima, S.; Tanigaki, K.; Hiura, H. *Nature* **1993**, *362*, 522.